Decentralized Direction-of-Arrival Estimation for Arbitrary Array Geometries

Wassim Suleiman
suleiman@spg.tu-darmstadt.de

Ansab Abdul Vaheed
ansabav@gmail.com

Marius Pesavento
pesavento@nt.tu-darmstadt.de

Abdelhak M. Zoubir
zoubir@spg.tu-darmstadt.de

***Abstract*—Direction-of-arrival (DOA) estimation in partly calibrated array composed of multiple fully calibrated subarrays is considered. The location of the sensors in the subarrays are assumed to be arbitrary, i.e., no specific subarray geometry is assumed. Using array interpolation, we extend the previously proposed decentralized ESPRIT algorithm (d-ESPRIT), originally designed for shift-invariance array geometries, to arbitrary array geometries. In our proposed algorithm, the array interpolation is carried out locally at the subarrays, thus, communication between the subarrays is required for DOA estimation but not for interpolation. Simulation results demonstrate that our proposed algorithm achieves better performance than the conventional ESPRIT algorithm in perturbed shift-invariance arrays.**

I. Introduction

DOA estimation using an array of sensors has a wide range of applications, e.g., radar, sonar, and seismic exploration [1], [2]. The MUSIC algorithm [3] is a subspace DOA estimation method which exhibits the super resolution property and is applicable in arbitrary array geometries as long as the array is fully calibrated, i.e., the absolute location of all sensors in the array is known. In the spectral MUSIC algorithm, DOA estimation is carried out in form of a line search, where the field of view is sampled at fine angular grid points, for which the MUSIC spectrum [3, Eq. 6] is computed. Grid points which correspond to the peaks in the MUSIC spectrum yield the DOA estimates. The major drawback of search-based DOA estimation algorithms as MUSIC is the high computational complexity required for the evaluation of the spatial spectrum.

To overcome this drawback, search-free DOA estimation algorithms, e.g., root-MUSIC [4] and ESPRIT [5], have been developed. Although computationally faster with improved performance, the root-MUSIC algorithm is only applicable in uniform linear array (ULA) geometries [4], [6]. Likewise, to achieve search-free DOA estimation, the ESPRIT algorithm restricts the array geometry to shift-invariance array structures.

In [7], a linear array interpolation has been proposed, with the objective to make search-free DOA estimation algorithms applicable to sensor arrays with arbitrary array geometries. Array interpolation is based on a mapping of the response of the true (i.e., physical) sensor array with arbitrary sensor locations to the response of a virtual array with desired geometry, such as a ULA or a shift-invariance array. Utilizing array interpolation, search-free DOA estimation is achieved in [7] using the interpolated root-MUSIC algorithm and in [8], [9] using the interpolated ESPRIT algorithm. The methods in [7]–[9] assume fully calibrated arrays, and they are performed in a centralized processing scheme.

Centralized processing, however, requires the collection of measurements from all sensors at a central processor (CP). A major drawback of centralized processing schemes with a single CP, is the existence of communication bottlenecks that generally emerge in large sensor networks with multi-hop communication [10], [11]. To overcome these drawbacks decentralized algorithms based on averaging consensus (AC) protocols have been introduced [15]–[17]. In AC protocols, an iterative fully decentralized calculation of the average of distributed scalars is carried out using only local communication between neighboring nodes. No CP is required in AC protocols, thus eliminating communication bottlenecks.

In large arrays, calibration is very difficult as different parts of the array may be widely separated. Hence in order to carry out DOA estimation, a common approach is to partition the large array of sensors into a set of smaller subarrays where the subarrays are considered as fully calibrated, and the displacements between the subarrays are considered to be unknown. Thus, the array is referred to as a partly calibrated array [5], [18]. Decentralized DOA estimation based on the AC protocol and the ESPRIT algorithm was introduced and analyzed in [11]–[14] for partly calibrated arrays. The resulting algorithm is referred to as the decentralized ESPRIT (d-ESPRIT). Similar to the conventional ESPRIT, the d-ESPRIT algorithm assumes shift-invariance arrays.

In this paper, we generalize the d-ESPRIT algorithm [11] to the case of arbitrary array geometries using array interpolation. In contrast to the approaches introduced in [7] and [9], in our interpolation approach we assume the array to be partly calibrated. Moreover, in our decentralized approach, the computation of the virtual array response is carried out locally at each subarray, thus, keeping the communication cost of the d-ESPRIT algorithm unchanged.

The remainder of this paper is organized as follows. In Section II, the signal model is introduced. The conventional ESPRIT [5] and d-ESPRIT [11] algorithms are briefly reviewed in Section III. In Section IV, array interpolation and the interpolated d-ESPRIT algorithm (ID-ESPRIT) for DOA estimation in arbitrary array geometries is introduced. In Section V, simulation results which demonstrate the performance of our proposed algorithm are presented.

In this paper, $(\cdot)^T$,$(\cdot)^H$ denote the transpose and complex conjugate operators, respectively. The $i\times i$ identity matrix and the operator which constructs diagonal matrix are expressed as $\boldsymbol{I}_i$ and diag$[\cdot]$, respectively. The expectation operator is denoted as $\mathbb{E}[\cdot]$, while $\jmath^2=-1$ is the imaginary unit.

II. Signal Model

Consider a planar array composed of M identical sensors. The array is partitioned into K subarrays where the kth subarray is comprised of M_k sensors, thus $M=\sum_{k=1}^{K} M_k$. The vector $\tilde{\boldsymbol{\xi}}_{k,m}=[\tilde{x}_{k,m},\tilde{y}_{k,m}]^T$ contains the x-y coordinates

978-0-9928-6265-7/16/$31.00 ©2016 IEEE

of the mth sensor in the kth subarray where the origin of the coordinate system for each subarray corresponds to its first sensor. The coordinate $\tilde{\boldsymbol{\xi}}_{k,m}$ (relative to the origin of the kth subarray) is considered to be known, i.e., the subarray is fully calibrated. However, displacements between the subarrays are assumed to be unknown, i.e., the whole array is partly calibrated [18]. Thus, the location of the first sensor in the kth subarray with respect to the first sensor in the first subarray, denoted as $\boldsymbol{\xi}_k = [x_k, y_k]$, is unknown.

Signals from L far-field narrow-band sources impinge onto the array from directions $\boldsymbol{\theta} = [\theta_1, \ldots, \theta_L]^T$ relative to the array broadside. The measurement model at time t is written as

$$\boldsymbol{z}_k(t) = \boldsymbol{A}_k(\boldsymbol{\theta}, \boldsymbol{\xi}_k)\boldsymbol{s}(t) + \boldsymbol{n}_k(t), \tag{1}$$

where $\boldsymbol{z}_k(t) \in \mathbb{C}^{M_k \times 1}$ is the received base-band signal vector at the kth subarray, $\boldsymbol{s}(t) \in \mathbb{C}^{L \times 1}$ is the signal vector of the L sources, and $\boldsymbol{n}_k(t) \in \mathbb{C}^{M_k \times 1}$ is the vector of temporally and spatially white complex circular Gaussian sensor noise. The steering matrix $\boldsymbol{A}_k$ can be factorized as

$$\boldsymbol{A}_k(\boldsymbol{\theta}, \boldsymbol{\xi}_k) = \boldsymbol{V}_k(\boldsymbol{\theta})\boldsymbol{\Xi}_k(\boldsymbol{\theta}, \boldsymbol{\xi}_k), \tag{2}$$

where the matrix $\boldsymbol{V}_k(\boldsymbol{\theta})$=$[\boldsymbol{v}_k(\theta_1), \ldots, \boldsymbol{v}_k(\theta_L)]$ is independent of the unknown displacements $\boldsymbol{\xi}_k$, $\boldsymbol{v}_k(\theta)$=$[1, \exp(\jmath\pi\tilde{\boldsymbol{\xi}}_{k,2}^T\boldsymbol{\nu}_\theta), \ldots, \exp(\jmath\pi\tilde{\boldsymbol{\xi}}_{k,M_k}^T\boldsymbol{\nu}_\theta)]^T$, $\boldsymbol{\nu}_\theta = [\sin\theta, \cos\theta]^T$, $\boldsymbol{\Xi}_k(\boldsymbol{\theta}, \boldsymbol{\xi}_k) = \mathrm{diag}[\exp(\jmath\pi\boldsymbol{\xi}_k^T\boldsymbol{\nu}_{\theta_1}), \ldots, \exp(\jmath\pi\boldsymbol{\xi}_k^T\boldsymbol{\nu}_{\theta_L})]$, and all distances are measured in half-wavelength.

Let $\boldsymbol{z}(t)$=$[\boldsymbol{z}_1^T(t), \ldots, \boldsymbol{z}_K^T(t)]^T$, $\boldsymbol{n}(t)$=$[\boldsymbol{n}_1^T(t), \ldots, \boldsymbol{n}_K^T(t)]$, and $\boldsymbol{A}(\boldsymbol{\theta}, \boldsymbol{\xi}) = [\boldsymbol{A}_1^T(\boldsymbol{\theta}, \boldsymbol{\xi}_1), \ldots, \boldsymbol{A}_K^T(\boldsymbol{\theta}, \boldsymbol{\xi}_K)]^T$, where $\boldsymbol{\xi} = [\boldsymbol{\xi}_1^T, \ldots, \boldsymbol{\xi}_K^T]^T$. Then, the measurement covariance matrix $\boldsymbol{R} = \mathbb{E}[\boldsymbol{z}(t)\boldsymbol{z}^H(t)]$ is given by

$$\boldsymbol{R} = \boldsymbol{A}(\boldsymbol{\theta}, \boldsymbol{\xi})\boldsymbol{P}\boldsymbol{A}^H(\boldsymbol{\theta}, \boldsymbol{\xi}) + \sigma^2\boldsymbol{I}_M, \tag{3}$$

where $\boldsymbol{P} = \mathbb{E}[\boldsymbol{s}(t)\boldsymbol{s}^H(t)]$ is the covariance matrix of the source signals and σ^2 is the noise variance. The eigendecomposition of the covariance matrix is expressed as

$$\boldsymbol{R} = \boldsymbol{U}_\mathrm{s}\boldsymbol{\Lambda}_\mathrm{s}\boldsymbol{U}_\mathrm{s}^H + \boldsymbol{U}_\mathrm{n}\boldsymbol{\Lambda}_\mathrm{n}\boldsymbol{U}_\mathrm{n}^H, \tag{4}$$

where $\boldsymbol{U}_\mathrm{s} = [\boldsymbol{u}_1, \ldots, \boldsymbol{u}_L]$, $\boldsymbol{U}_\mathrm{n} = [\boldsymbol{u}_{L+1}, \ldots, \boldsymbol{u}_M]$ denote the signal and noise subspace matrices, respectively, $\boldsymbol{\Lambda}_\mathrm{s} = \mathrm{diag}[\lambda_1, \ldots, \lambda_L]$, $\boldsymbol{\Lambda}_\mathrm{n} = \mathrm{diag}[\lambda_{L+1}, \ldots, \lambda_M]$, and $\boldsymbol{u}_1, \ldots, \boldsymbol{u}_M$ are the eigenvectors of the matrix $\boldsymbol{R}$ corresponding to the eigenvalues ordered as $\lambda_1 \geq \ldots \geq \lambda_L > \lambda_{L+1} = \ldots = \lambda_M = \sigma^2$.

The sample estimate of the covariance matrix is given by

$$\hat{\boldsymbol{R}} = \frac{1}{N}\sum_{t=1}^{N}\boldsymbol{z}(t)\boldsymbol{z}^H(t), \tag{5}$$

where N is the number of snapshots of the array output. Let $\hat{\boldsymbol{U}}_\mathrm{s}$, $\hat{\boldsymbol{\Lambda}}_\mathrm{s}$, $\hat{\boldsymbol{U}}_\mathrm{n}$, $\hat{\boldsymbol{\Lambda}}_\mathrm{n}$, $\hat{\boldsymbol{u}}_i$, $\hat{\lambda}_i$ obtained from the eigendecomposition of the matrix $\hat{\boldsymbol{R}}$ be the estimates of $\boldsymbol{U}_\mathrm{s}$, $\boldsymbol{\Lambda}_\mathrm{s}$, $\boldsymbol{U}_\mathrm{n}$, $\boldsymbol{\Lambda}_\mathrm{n}$, $\boldsymbol{u}_i$, λ_i, respectively, for $i = 1, \ldots, M$.

III. The Decentralized ESPRIT Algorithm

In this section, the conventional ESPRIT algorithm is revisited and the AC protocol is described. Then, the d-ESPRIT algorithm which is based on the decentralized eigendecomposition of the sample covariance matrix using the decentralized power method (d-PM) is reviewed.

A. The Conventional ESPRIT Algorithm

The conventional ESPRIT algorithm introduced in [5] performs search-free DOA estimation. However, it requires the array to be shift-invariance, i.e., the whole array is partitioned in upper and lower groups of sensors, where the lower groups of sensors correspond to the upper groups of sensor displaced by a shift of d.

Let $\boldsymbol{e}_1, \ldots, \boldsymbol{e}_M$ be the columns of the $M \times M$ identity matrix $\boldsymbol{I}_M$ and let $\tilde{M}$ denote the number of sensors in the upper and lower groups of sensors. Then, the upper and lower selection matrices are defined as $\overline{\boldsymbol{J}} = [\boldsymbol{e}_{i_1}, \ldots, \boldsymbol{e}_{i_{\tilde{M}}}]^T$ and $\underline{\boldsymbol{J}} = [\boldsymbol{e}_{j_1}, \ldots, \boldsymbol{e}_{j_{\tilde{M}}}]^T$, respectively, where $i_1, \ldots, i_{\tilde{M}}$ and $j_1, \ldots, j_{\tilde{M}}$ are the indices of the sensors in the upper and lower groups, respectively. Based on the selection matrices $\overline{\boldsymbol{J}}$ and $\underline{\boldsymbol{J}}$, we define

$$\hat{\overline{\boldsymbol{U}}}_\mathrm{s} = \overline{\boldsymbol{J}}\hat{\boldsymbol{U}}_\mathrm{s}, \quad \hat{\underline{\boldsymbol{U}}}_\mathrm{s} = \underline{\boldsymbol{J}}\hat{\boldsymbol{U}}_\mathrm{s}. \tag{6}$$

In [5], it has been shown that the DOAs can be estimated as

$$\theta_l = \sin^{-1}(\arg(\psi_l)/\pi d), \tag{7}$$

where ψ_l, $l = 1, \ldots, L$ are the eigenvalues of the $L \times L$ matrix

$$\boldsymbol{\psi} = (\hat{\overline{\boldsymbol{U}}}_\mathrm{s}^H\hat{\overline{\boldsymbol{U}}}_\mathrm{s})^{-1}\hat{\overline{\boldsymbol{U}}}_\mathrm{s}^H\hat{\underline{\boldsymbol{U}}}_\mathrm{s}. \tag{8}$$

B. The Averaging Consensus Protocol

Let $y_1, \ldots, y_K$ be K scalars distributed over the network of K subarrays where the kth subarray stores the kth scalar value y_k. Then, the AC protocol can be used iteratively to compute the average of these scalars, where in the pth iteration of the AC protocol, the kth node updates its value of the average $y_k^{(p)}$ as follows:

$$y_k^{(p)} = w_{k,k}y_k^{(p-1)} + \sum_{i \in \mathcal{N}_k} w_{i,k}y_i^{(p-1)}, \tag{9}$$

where $\mathcal{N}_k$ denotes the set of neighbors of the kth subarray and $w_{i,k}$ is the weighting factor associated with the communication link between the subarrays i and k. The weighting factors satisfy $w_{i,k} = 0$ when $i \notin \mathcal{N}_k$. The AC iteration is initialized with $y_k^{(0)} = y_k$. The update iteration in Eq. (9) can be written as

$$\boldsymbol{y}^{(p)} = \boldsymbol{W}\boldsymbol{y}^{(p-1)} = \boldsymbol{W}^2\boldsymbol{y}^{(p-2)} = \ldots = \boldsymbol{W}^p\boldsymbol{y}^{(0)}, \tag{10}$$

where $\boldsymbol{W}$ denotes the matrix with entries $[\boldsymbol{W}]_{i,j} = w_{i,j}$ for $i, j = 1, \ldots, K$ and $\boldsymbol{y}^{(p)} = [y_1^{(p)}, \ldots, y_K^{(p)}]^T$. For further details concerning the AC protocol and the optimal selection of the weighting factors we refer to [15].

C. The Decentralized ESPRIT Algorithm

The d-ESPRIT algorithm, introduced in [12], utilizes the decentralized power method (d-PM), which is proposed in [10], to estimate the signal subspace $\hat{\boldsymbol{U}}_\mathrm{s}$. Similar to the conventional PM [19], the lth eigenvector of the sample covariance matrix $\hat{\boldsymbol{R}}$ at the qth iteration of the d-PM is computed as

$$\hat{\boldsymbol{u}}_l^{(q)} = (\boldsymbol{I}_M - \hat{\boldsymbol{U}}_{l-1}\hat{\boldsymbol{U}}_{l-1}^H)\hat{\boldsymbol{u}}_l^{'(q-1)}, \tag{11}$$

where $\hat{\boldsymbol{u}}_l^{(q-1)}$ is the lth eigenvector computed in the preceding iteration $(q-1)$, $\hat{\boldsymbol{u}}_l^{'(q-1)} = \hat{\boldsymbol{R}}\hat{\boldsymbol{u}}_l^{(q-1)}$ is an intermediate vector, and $\hat{\boldsymbol{U}}_{l-1} = [\hat{\boldsymbol{u}}_1, \ldots, \hat{\boldsymbol{u}}_{l-1}]$ is the concatenation of $(l-1)$ eigenvectors of $\hat{\boldsymbol{R}}$ computed previously. The vector $\hat{\boldsymbol{u}}_l^{(0)}$ is

chosen randomly. The main idea of the d-PM is to partition the lth eigenvector as $\hat{\boldsymbol{u}}_l^{(q)} = [\hat{\boldsymbol{u}}_{l,1}^{(q)T}, \ldots, \hat{\boldsymbol{u}}_{l,K}^{(q)T}]^T$, where the kth subarray updates and stores only the kth part, $\hat{\boldsymbol{u}}_{l,k}^{(q)} \in \mathbb{C}^{M_k \times 1}$ of the vector $\hat{\boldsymbol{u}}_l^{(q)}$. The kth part of the vector $\hat{\boldsymbol{u}}_l^{'(q-1)}$ can be written as $\hat{\boldsymbol{u}}_{l,k}^{'(q-1)} = \frac{1}{N}\sum_{t=1}^{N} \boldsymbol{z}_k(t)\tilde{z}_{t,l}^{(q-1)}$, where $\tilde{z}_{t,l}^{(q-1)} = \boldsymbol{z}^H(t)\hat{\boldsymbol{u}}_l^{(q-1)}$. The vector $\hat{\boldsymbol{u}}_{l,k}^{'(q-1)}$ can be computed locally if the scalars $\left\{\tilde{z}_{t,l}^{(q-1)}\right\}_{t=1}^{N}$ are available at the kth subarray. This is achieved using the AC protocol with P iterations since $\tilde{z}_{t,l}^{(q-1)}$ can be written as an average of scalars which are distributed among the subarrays as $\tilde{z}_{t,l}^{(q-1)} = K(\frac{1}{K}\sum_{k=1}^{K} \boldsymbol{z}_k^H(t)\hat{\boldsymbol{u}}_{l,k}^{(q-1)})$. The product $\hat{\boldsymbol{U}}_{l-1}\hat{\boldsymbol{U}}_{l-1}^H\hat{\boldsymbol{u}}_l^{'(q-1)}$ in Eq. (11) can also be computed using the AC protocol, see [10] for details. After a sufficiently large[1] number of PM iterations Q, the vector $\hat{\boldsymbol{u}}_l^{(Q)}$ is normalized to obtain the estimate of the lth eigenvector of $\hat{\boldsymbol{R}}$, i.e., $\hat{\boldsymbol{u}}_l = \hat{\boldsymbol{u}}_l^{(q)}/\|\hat{\boldsymbol{u}}_l^{(q)}\|$. The decentralized estimate of the signal subspace $\hat{\boldsymbol{U}}_{\mathrm{s}}$ which we obtain from the d-PM is distributed among all the subarrays where the kth subarray stores only the M_k rows of the matrix $\hat{\boldsymbol{U}}_{\mathrm{s}}$ which correspond to its measurements. Thus, the matrix $\hat{\boldsymbol{U}}_{\mathrm{s}}$ is partitioned as

$$\hat{\boldsymbol{U}}_{\mathrm{s}} = [\hat{\boldsymbol{U}}_{\mathrm{s},1}^T, \ldots, \hat{\boldsymbol{U}}_{\mathrm{s},K}^T]^T. \tag{12}$$

In [11], it is shown that the matrix $\boldsymbol{\psi}$, defined in Eq. (8), can be computed in a decentralized fashion using the AC protocol such that each subarray has access to this matrix. Consequently, each subarray is able to estimate the DOAs locally.

IV. The Decentralized ESPRIT Algorithm for Arbitrary Array Geometries

In this section, the general approach for linear interpolated array is briefly reviewed. Then, the interpolated decentralized ESPRIT algorithm (ID-ESPRIT) is introduced.

A. Array Interpolation

In the linear interpolation technique [7], the virtual array manifold is obtained by linear transformation of the true array manifold over a given angular sector. Let Θ denote the grid of G directions which is obtained by sampling the field-of-view at directions $\Theta = [\tilde{\theta}_1, \ldots, \tilde{\theta}_G]$, where $\tilde{\theta}_g \in [-90, 90]$, for $g = 1, \ldots, G$. Then, assuming a fully-calibrated array as in [7], the virtual array manifold $\breve{\boldsymbol{A}}(\Theta)$ can be written as

$$\breve{\boldsymbol{A}}(\Theta) = \boldsymbol{B}\boldsymbol{A}(\Theta), \tag{13}$$

where $\boldsymbol{B}$ is the transformation matrix and $\boldsymbol{A}(\Theta)$ is the true array manifold computed at the grid points Θ. The structure of the virtual array is chosen according to the DOA estimation algorithm that is applied in the estimation. For example, in [7], the virtual array geometry is chosen as a ULA as the root-MUSIC algorithm is applied to the resulting transformed measurements, while in [8] and [9] the virtual array is chosen as a shifted version of the true array and the ESPRIT algorithm is used. Since both matrices $\breve{\boldsymbol{A}}(\Theta)$ and $\boldsymbol{A}(\Theta)$ are known, the transformation matrix $\boldsymbol{B}$ can be computed from Eq. (13) using the Least Squares (LS) method. More sophisticated interpolation methods are known, see e.g., [20].

[1] In simulations, we observed that a number of $Q = 10$ PM iterations is sufficient.

B. Interpolated Decentralized ESPRIT

Our aim is to generalize the d-ESPRIT [12] algorithm to arbitrary array geometries. Since in the d-ESPRIT algorithm unknown displacements between the subarrays are assumed, the true array manifold is not completely known as a function of the DOAs, i.e., both matrices $\boldsymbol{A}$ and $\breve{\boldsymbol{A}}$ in Eq. (13) are not fully known. Nevertheless, in the sequel, we show that array interpolation can still be applied to our scenario.

As in [8], [9], we assume that the virtual array manifold is a shifted version of the true array manifold which can be expressed at the kth subarray as

$$\breve{\boldsymbol{A}}_k(\Theta, \boldsymbol{\xi}) = \boldsymbol{A}_k(\Theta, \boldsymbol{\xi})\boldsymbol{\phi}(\Theta, d), \tag{14}$$

where $\boldsymbol{\phi}(\Theta, d) = \mathrm{diag}[\exp(j\pi d \sin\tilde{\theta}_1), \ldots, \exp(j\pi d \sin\tilde{\theta}_G)]$ and d is the shift between the true and the virtual subarray measured in half-wavelength. Substituting Eq. (14) in Eq. (13), yields

$$\boldsymbol{A}_k(\Theta, \boldsymbol{\xi})\boldsymbol{\phi}(\Theta, d) = \boldsymbol{B}_k\boldsymbol{A}_k(\Theta, \boldsymbol{\xi}). \tag{15}$$

Using the factorization (1) in Eq. (15), we obtain

$$\boldsymbol{V}_k(\Theta)\Xi_k(\Theta, \boldsymbol{\xi}_k)\boldsymbol{\phi}(\Theta, d) = \boldsymbol{B}_k\boldsymbol{V}_k(\Theta)\Xi_k(\Theta, \boldsymbol{\xi}_k). \tag{16}$$

Noting that $\Xi_k(\Theta, \boldsymbol{\xi}_k)\boldsymbol{\phi}(\Theta, d) = \boldsymbol{\phi}(\Theta, d)\Xi_k(\Theta, \boldsymbol{\xi}_k)$ since both matrices $\Xi_k(\Theta, \boldsymbol{\xi}_k)$ and $\boldsymbol{\phi}(\Theta, d)$ are diagonal and invertible Eq. (16) is reduced to

$$\boldsymbol{V}_k(\Theta)\boldsymbol{\phi}(\Theta, d) = \boldsymbol{B}_k\boldsymbol{V}_k(\Theta), \tag{17}$$

where both matrices $\boldsymbol{V}_k(\Theta)$ and $\boldsymbol{\phi}(\Theta, d)$ are known. Thus, the transformation matrix $\boldsymbol{B}_k$ can be computed using the LS method locally at the kth subarray, since the matrix $\boldsymbol{B}_k$ depends only on the (locally available) matrices $\boldsymbol{V}_k(\Theta)$ and $\boldsymbol{\phi}(\Theta, d)$. Note that the matrix $\boldsymbol{B}_k$ is computed only once, unless the physical subarray geometry has been modified.

We point out that, the transformation introduced in Eq. (15) can also be applied jointly to the whole array, i.e., as $\boldsymbol{A}(\Theta, \boldsymbol{\xi})\boldsymbol{\phi}(\Theta, d) = \boldsymbol{B}\boldsymbol{A}(\Theta, \boldsymbol{\xi})$, which due to the increased number of interpolation parameters, yields improved interpolation quality. However, the resulting interpolation matrix $\boldsymbol{B}$ depends on the geometry of all the subarrays through the matrices $\boldsymbol{V}_1(\Theta), \ldots, \boldsymbol{V}_K(\Theta)$ and, thus, it cannot be computed locally. Consequently, to avoid the communication load associated with the joint interpolation, we use the local interpolation in Eq. (15).

The ESPRIT algorithm [5] can be generalized to arbitrary array geometries using the interpolation matrices $\boldsymbol{B}_1, \ldots, \boldsymbol{B}_K$ and the estimated signal subspace matrices $\hat{\boldsymbol{U}}_{\mathrm{s},1}, \ldots, \hat{\boldsymbol{U}}_{\mathrm{s},K}$ as follows. Firstly, the signal subspace matrices of the virtual array is computed as

$$\hat{\breve{\boldsymbol{U}}}_{\mathrm{s},k} = \boldsymbol{B}_k\hat{\boldsymbol{U}}_{\mathrm{s},k}, \tag{18}$$

for $k = 1, \ldots, K$. Secondly, since the virtual subspace matrix computed in Eq. (18) corresponds to the shifted version of the real array, analogous to the ESPRIT algorithm, the matrix $\boldsymbol{\psi}$ in Eq. (8) can be estimated as

$$\hat{\boldsymbol{\psi}} = (\hat{\boldsymbol{U}}_{\mathrm{s}}^H\hat{\boldsymbol{U}}_{\mathrm{s}})^{-1}\hat{\boldsymbol{U}}_{\mathrm{s}}^H\hat{\breve{\boldsymbol{U}}}_{\mathrm{s}}, \tag{19}$$

where similar to Eq. (12) the resulting virtual subspace matrix is partitioned as $\hat{\breve{\boldsymbol{U}}}_{\mathrm{s}} = [\hat{\breve{\boldsymbol{U}}}_{\mathrm{s},1}^T, \ldots, \hat{\breve{\boldsymbol{U}}}_{\mathrm{s},K}^T]^T$. The ID-ESPRIT is summarized in Algorithm 1.

Algorithm 1 summary of the ID-ESPRIT algorithm

Step 1: Estimate the signal subspace $\hat{\boldsymbol{U}}_{\mathrm{s}}$ in a fully decentralized fashion using the d-PM as in [10].

Step 2: Locally compute $\hat{\mathring{\boldsymbol{U}}}_{\mathrm{s},k} = \boldsymbol{B}_k \hat{\boldsymbol{U}}_{\mathrm{s},k}$ at each subarray.

Step 3: Compute the matrix $\hat{\boldsymbol{\psi}}$ in a fully decentralized fashion as introduced in [11] and [12].

Step 4: Estimate the DOAs locally at each subarray from the eigenvalues of $\hat{\boldsymbol{\psi}}$ using Eq. (7).

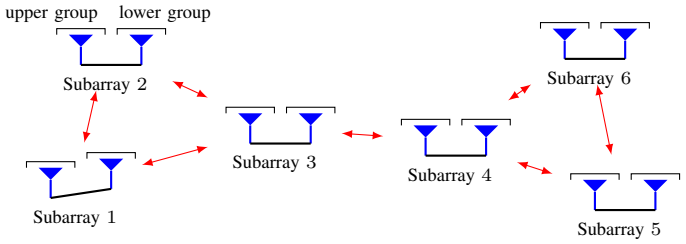

Fig. 1. Scenario 1: the array topology possesses the shift-invariance property, however, the location of the second sensor of the first subarray is perturbed.

V. Simulation Results

An array composed of $K = 6$ subarrays, where each subarray consists of two sensors, i.e., M=12, is used to analyze the performance of the ID-ESPRIT algorithm in two scenarios.

In the first scenario, which is demonstrated in Fig. 1, the location of the sensors is chosen such that the array exhibits the shift-invariance property. Then, the location of the second sensor of the first subarray is randomly perturbed to introduce small displacements around the nominal (shift-invariance) locations. The locations of the sensors of the 6 subarrays measured in half-wavelength are $\{(0,0),\ (1,0.05)\}$, $\{(0.3,0.7),\ (1.3,0.7)\}$, $\{(2.0,0.4),\ (3.0,0.4)\}$, $\{(5.0,0.2),\ (6.0,0.2)\}$, $\{(7.0,-0.2),\ (8.0,-0.2)\}$, and $\{(6.0,0.8),\ (7.0,0.8)\}$. Note that if the second sensor of the first subarray is shifted by -0.05 at the y axis, then the array would become shift-invariance.

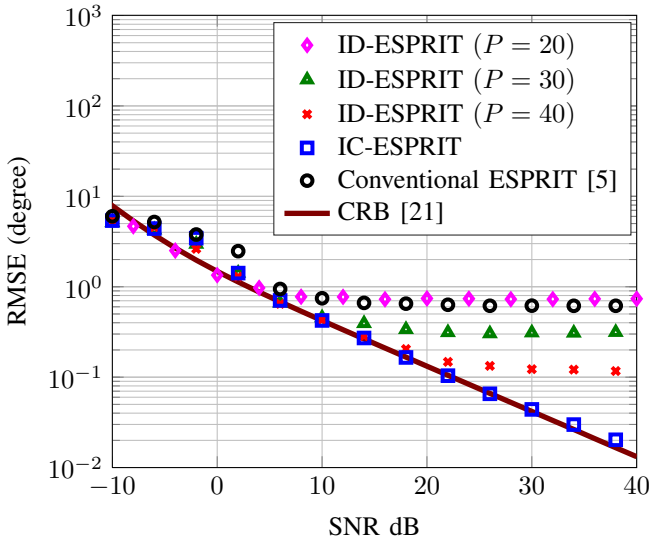

Fig. 2. RMSE as a function of SNR for Scenario 1 where $N = 100$.

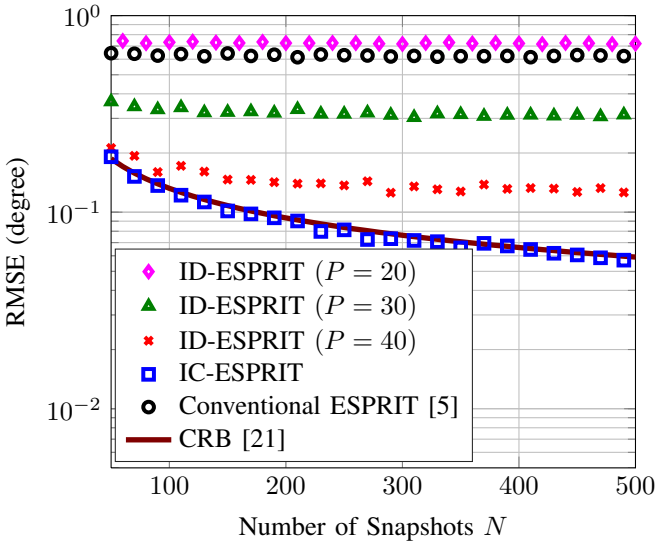

Fig. 3. RMSE as a function of N for Scenario 1 where SNR= 20 dB.

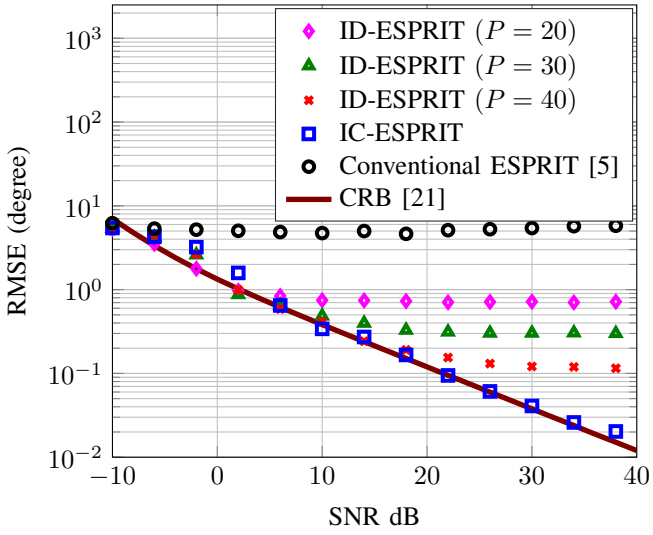

Fig. 4. RMSE as a function of SNR for Scenario 2 where $N = 100$.

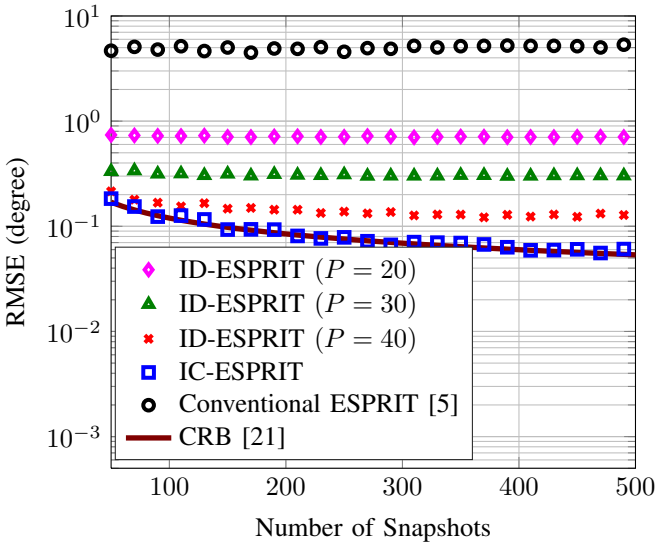

Fig. 5. RMSE as a function of N for Scenario 2 where SNR= 20 dB.

In the second scenario, the locations of the second sensor in all subarrays are selected arbitrarily. The locations of the sensors of the 6 subarrays measured in half-wavelength in this scenario are $\{(0,0),\ (0.9,0.1)\}$, $\{(0.3,0.7),\ (1.4,0.69)\}$, $\{(2.0,0.4),\ (2.8,0.42)\}$, $\{(5.0,0.2),\ (6.0,0.15)\}$, $\{(7.0,-0.2),\ (8.0,-0.4)\}$, and $\{(6.0,0.8),\ (7.6,1.0)\}$.

In both scenarios, signals from $L = 2$ far-field narrowband sources impinge onto the subarrays from directions -4° and -0°. The root mean square error (RMSE) of the ID-ESPRIT algorithm is computed over 100 Monte Carlo runs for 3 different numbers of AC iterations, $P = 20, 30$, and 40, in both scenarios. The weighting scheme in [15, Section 4.2] is used to compute the entries of the averaging matrix $\boldsymbol{W}$, where the subarrays linked with (red) arrows in Fig. 1 are considered to be able to directly communicate with each other. The following parameters are selected for the ID-ESPRIT algorithm: $d = 1$, $Q = 10$, and the sampling step size is 0.1° in the grid Θ. Moreover, the empirical performance of the conventional ESPRIT and the interpolated conventional ESPRIT (IC-ESPRIT) algorithms and the Cramer Rao bound (CRB) [21] is plotted for benchmarking, in both scenarios.

A. Scenario 1

Simulation results for Scenario 1 are shown in Fig. 2 and Fig. 3. In Fig. 2, the RMSE is plotted as a function of the signal-to-noise ratio (SNR) where the number of snapshots is fixed to $N = 100$. It can be observed in this figure that the conventional ESPRIT algorithm does not achieve the CRB due to the perturbation in the subarray structure. The IC-ESPRIT algorithm achieves the CRB since it does not assume a shift-invariance array. The proposed ID-ESPRIT algorithm achieves a performance similar to the conventional ESPRIT for $P = 20$ and achieves a better performance than the conventional ESPRIT for $P = 30$ and 40. Observe that at high SNRs the performance of the ID-ESPRIT algorithm does not improve with SNR, due to the errors introduced by the finite number of AC iterations. This behaviour is noticeable in the d-ESPRIT algorithm and has been analyzed in [11].

Fig. 3 displays the RMSE as a function of the number of snapshots N while the SNR is fixed to 20 dB. Similar to Fig. 2, it can be observed that the ID-ESPRIT algorithm perform better than the conventional ESPRIT as it does not depend on the assumption of shift-invariance arrays.

B. Scenario 2

The simulation results for the second scenario are demonstrated in Fig. 4 and Fig. 5. It can be observed in both figures that the RMSE of the conventional ESPRIT algorithm is very high, since in this scenario the conventional ESPRIT algorithm is not able to resolve the two sources. However, the IC-ESPRIT and the ID-ESPRIT algorithms achieve performance similar to Scenario 1, since they both do not rely on the assumption of shift-invariance arrays.

VI. Conclusion

A search-free decentralized DOA estimation algorithm is introduced which is applicable to partly calibrated arrays with an arbitrarily known subarray geometry. This is achieved by applying array interpolation in the decentralized ESPRIT algorithm. We have shown by simulations that our proposed algorithm achieves better performance than the conventional ESPRIT if the array has a perturbed shift-invariance geometry.

Acknowledgment

The project ADEL acknowledges the financial support of the Seventh Framework Programme for Research of the European Commission under grant number: 619647.

References

[1] H. L. Van Trees, *Detection, estimation, and modulation theory, optimum array processing*. John Wiley & Sons, 2004.

[2] H. Krim and M. Viberg, "Two decades of array signal processing research: the parametric approach," *IEEE Signal Processing Magazine*, vol. 13, no. 4, pp. 67–94, 1996.

[3] R. O. Schmidt, "Multiple emitter location and signal parameter estimation," *IEEE Transactions on Antennas and Propagation*, vol. 34, no. 3, pp. 276–280, 1986.

[4] A. J. Barabell, "Improving the resolution performance of eigenstructure-based direction-finding algorithms," in *IEEE International Conference on Acoustics, Speech, and Signal Processing (ICASSP)*, vol. 8, 1983, pp. 336–339.

[5] R. Roy and T. Kailath, "ESPRIT-Estimation of Signal Parameters via Rotational Invariance Techniques," *IEEE Transactions on Acoustics, Speech and Signal Processing*, vol. 37, no. 7, pp. 984–995, 1989.

[6] M. Pesavento, A. B. Gershman, and M. Haardt, "Unitary root-MUSIC with a real-valued eigendecomposition: A theoretical and experimental performance study," *IEEE Transactions on Signal Processing*, vol. 48, no. 5, pp. 1306–1314, 2000.

[7] B. Friedlander, "Direction finding using an interpolated array," *IEEE Signal Process Letters*, vol. 5, pp. 2951–2954, 1990.

[8] A. J. Weiss and M. Gavish, "The interpolated ESPRIT algorithm for direction finding," in *17th Convention of Electrical and Electronics Engineers in Israel*, 1991, pp. 361–364.

[9] M. Bühren, M. Pesavento, and J. F. Böhme, "A new approach to array interpolation by generation of artificial shift invariances: interpolated ESPRIT," in *IEEE International Conference on Acoustics, Speech, and Signal Processing (ICASSP)*, vol. 5, 2003, pp. V–205.

[10] A. Scaglione, R. Pagliari, and H. Krim, "The decentralized estimation of the sample covariance," in *42nd Asilomar Conference on Signals, Systems and Computers*, 2008, pp. 1722–1726.

[11] W. Suleiman, M. Pesavento, and A. M. Zoubir, "Performance analysis of the decentralized eigendecomposition and ESPRIT algorithm," *IEEE Transactions on Signal Processing*, vol. 64, no. 9, pp. 2375–2386, May 2016.

[12] W. Suleiman, M. Pesavento, and A. Zoubir, "Decentralized direction finding using partly calibrated arrays," in *Proceedings of the 21st European Signal Processing Conference (EUSIPCO)*, 2013, pp. 1–5.

[13] W. Suleiman, M. Pesavento, and A. M. Zoubir, "Decentralized cooperative DOA tracking using non-hermitian generalized eigendecomposition," in *European Signal Processing Conference (EUSIPCO)*, 2015, pp. 2626–2630.

[14] W. Suleiman, P. Parvazi, M. Pesavento, and A. Zoubir, "Decentralized direction finding using Lanczos method," in *IEEE Sensor Array and Multichannel Signal Processing Workshop (SAM)*, 2014, pp. 9–12.

[15] L. Xiao and S. Boyd, "Fast linear iterations for distributed averaging," *Systems & Control Letters*, vol. 53, no. 1, pp. 65–78, 2004.

[16] R. Olfati-Saber, A. Fax, and R. M. Murray, "Consensus and cooperation in networked multi-agent systems," *Proceedings of the IEEE*, vol. 95, no. 1, pp. 215–233, 2007.

[17] M. H. DeGroot, "Reaching a consensus," *Journal of the American Statistical Association*, vol. 69, no. 345, pp. 118–121, 1974.

[18] M. Pesavento, A. B. Gershman, and K. M. Wong, "Direction finding in partly calibrated sensor arrays composed of multiple subarrays," *IEEE Transactions on Signal Processing*, vol. 50, no. 9, pp. 2103–2115, 2002.

[19] G. H. Golub and C. F. Van Loan, "Matrix computations. johns hopkins studies in the mathematical sciences," 1996.

[20] M. Pesavento, A. B. Gershman, and Z.-Q. Luo, "Robust array interpolation using second-order cone programming," *IEEE Signal Processing Letters*, vol. 9, no. 1, pp. 8–11, 2002.

[21] C. M. S. See and A. B. Gershman, "Direction-of-arrival estimation in partly calibrated subarray-based sensor arrays," *IEEE Transactions on Signal Processing*, vol. 52, no. 2, pp. 329–338, 2004.